

# Clutter-free radar for cars

by J. Shefer, R. J. Klensch, G. Kaplan and H. C. Johnson

RCA Laboratories, New Jersey

**A radar system using second harmonic reflection that monitors the distance and closing rate of the car in front as well as the ground speed of the driver's car but remains immune to "blinding" and "clutter" from surrounding objects.**

During 1970, in the USA, there were 12.3 million collisions involving two or more vehicles. Of this number, 3.8 million, or close to one-third, were rear-end collisions.<sup>1</sup> An experimental car radar has been demonstrated which is designed to avoid rear-end collisions. A completely passive reflector, mounted on the back of vehicles, returns the second harmonic of the frequency transmitted from the trailing vehicle. The radar is immune to clutter since its receiver is tuned to the second harmonic frequency only. It is also immune to blinding by cars travelling in the opposite direction, as well as to other interference problems inherent in a "dense" environment.

## System considerations

RCA Laboratories have developed a radar system that will aid the driver in maintaining a safe distance from the car in front by constantly monitoring the distance and the closing rate, as well as his own ground speed. The driver would be warned by sound or light signals whenever the combination of these parameters indicates that the separation between his car and the car in front becomes unsafe. As a further step in the system's development, the brakes would at the same time be activated automatically. Throttle control can eventually be added for completely automated headway control.

A viable radar for cars on highways must first be immune to clutter, which includes reflections from the roadway, trees, highway signs, overpasses, bridges, and similar highway fixtures. The seriousness of clutter can be assessed when it is recognized that the radar cross-section of an overhead sign can be 30dB larger than the radar cross-section of the back of a small car. Other car radar systems try to cope with this problem by excluding any returns from objects that are stationary with respect to the ground. That kind of processing does eliminate clutter from stationary objects. Unfortunately, it also eliminates the return from a car standing in one's own lane. This is a serious deficiency, especially since a majority of all rear-end collisions occur at a time when the car in front has completely

stopped. When we add to the picture a large number of other cars carrying the same kind of radar and travelling in both directions of a highway, a whole new family of mutual interference problems arise. These can be characterized as blinding, masking, and cross-talk types of interference, which can cause false alarms or mask true alarms in conventional radar systems. In the harmonic radar system, however, they have been completely eliminated. Minimizing the incidence of false alarms is of prime importance if automobile radar systems are ever to become a reality. When false alarms occur more often than at a very low threshold rate, users are likely to lose faith in the system and either override it or shut it off completely.

## The harmonic radar concept

The radar receiver shown in Fig. 1 is tuned to the second harmonic of the transmitted frequency and the car in front is equipped with a special reflector that efficiently returns the second harmonic only. (In extensive testing so far we have not found any natural objects that will produce a detectable second harmonic frequency.) Thus clutter is eliminated because the sources, such as signs and overpasses do not produce radar echoes at the second harmonic. Blinding is eliminated because all radar receivers respond only to signals

at the second harmonic of the transmitted frequency.

## Blinding interference

Car A in Fig. 2 is travelling behind car E, with its conventional radar measuring distance to car E. Car D, going in the opposite direction, will deliver an enormously large signal to car A's receiver, compared with the reflection from car E. Quantitatively, the blinding signal can be 50dB or 60dB higher than the echo being looked for. This blinding transmission will therefore be seen from a long distance ahead and may cause a false alarm, as well as saturate the receiver of car A. The sidelobes from cars B and C may have the same effect. In the harmonic radar system, however, the receiver of car A will reject all signals other than the second harmonic of its transmitted frequency.

## Cross-talk interference

Indicated in Fig. 3 is another kind of interference, inherent in conventional radar, which may be called cross-talk interference. Car C in Fig. 3(a) may receive a false alarm even though it is in no danger of running into car B. With a harmonic radar, as in Fig. 3(b), the return signal is shaped into a well-defined beam, covering the width of one lane only.

In the situation on a curve, as in Fig. 4(a),

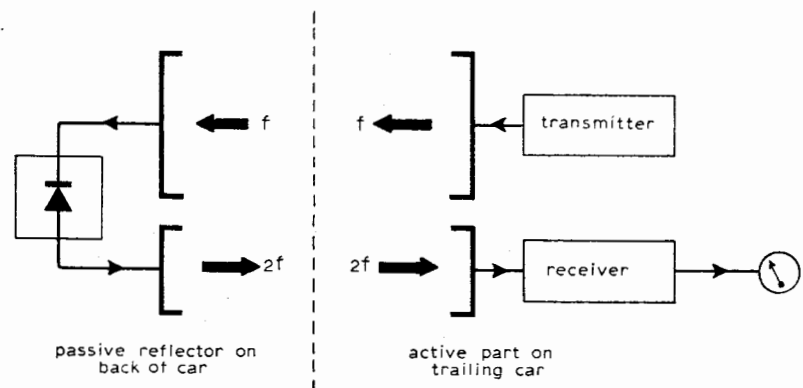


Fig. 1. Harmonic radar configuration.

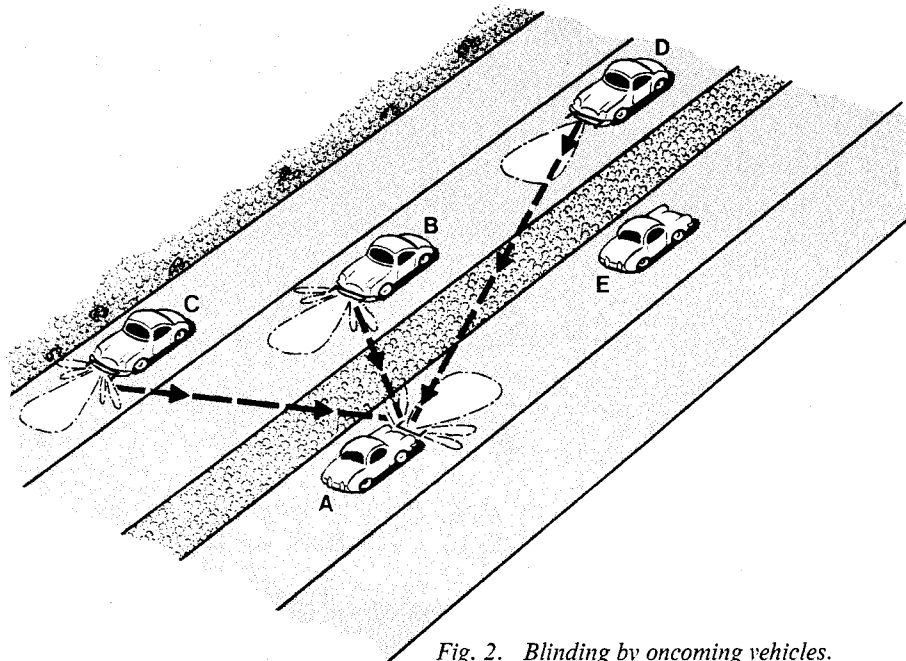


Fig. 2. Blinding by oncoming vehicles.

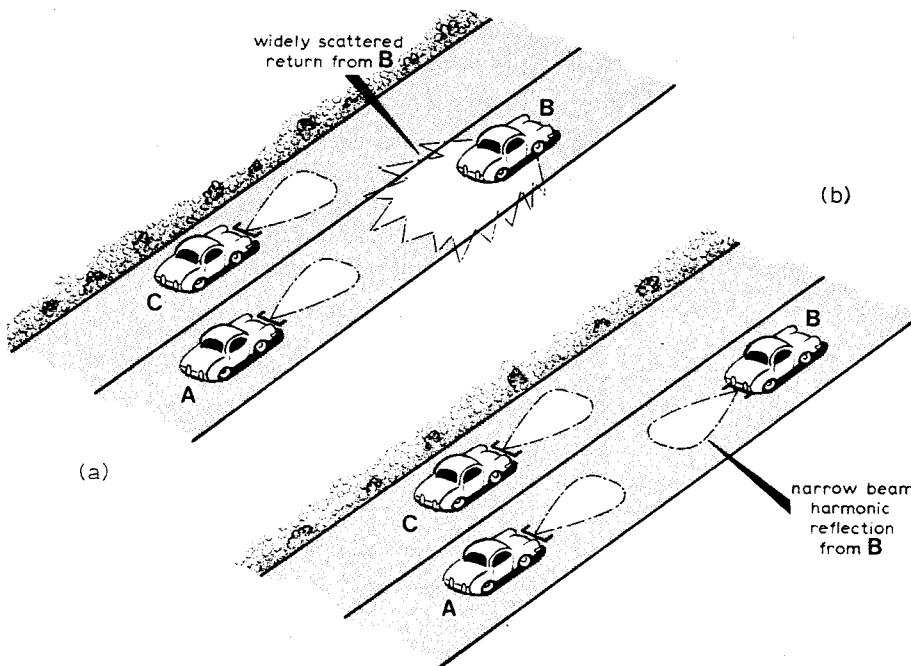


Fig. 3. Conventional versus harmonic radar: "cross talk" from adjacent lanes.

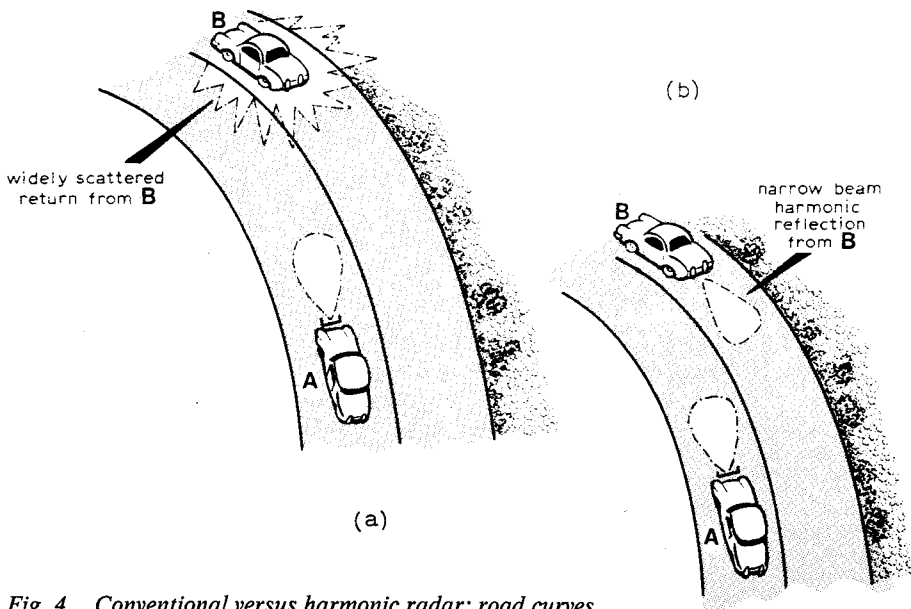


Fig. 4. Conventional versus harmonic radar: road curves.

quite evidently we do not need a third car to produce a false alarm. The skin of car B will respond to the transmission from a fundamental radar and may cause a false alarm at car A. Fig. 4(b) shows that with a well-defined narrow beam reflected from car B, if any reflection occurs at all, the possibility of a false alarm is drastically reduced.

**Masking interference**

Illustrated in Fig. 5 is yet another problem inherent in a conventional radar which uses the car's body as the reflector. Radar cross-sections of rears of cars can vary tremendously: the back of a lorry may have a radar cross-section several hundred times larger than a small car. The effect is then the masking of the desired return from a close vehicle by a larger vehicle much farther down the road. With the harmonic radar, all radar cross-sections of reflectors are the same, unless designed otherwise. If all reflectors are mounted at a standard height, only the nearest reflector can be "seen" while all others will be blocked.

The radar system described in this paper is unique in its ability to eliminate false targets and clutter, in its immunity to blinding by radars of similarly equipped vehicles, and in its potential of providing automatic braking for specifically "tagged" objects, such as known off-highway collision hazards or wrong-way entrances to one-way streets and highway access ramps.

When in general use, it also has the potential for safely providing higher traffic packing densities without running the risks of massive "pile-ups".

Although it is a co-operative system, in that all vehicles must carry the harmonic reflector, the reflector is completely passive, quite inexpensive in mass production, and can easily be fitted on existing vehicles. The co-operation required is not more burdensome than the requirement for red tail-light assemblies: and the purpose is the same—to aid in preventing collisions.

The radar uses solid-state components throughout, and is easily adaptable to integration and printed circuit techniques. It uses a frequency spectrum region that is still not crowded and, with a power density over the antenna aperture of 0.15mW/cm<sup>2</sup>, it does not constitute a radiation hazard even in the immediate vicinity of the radar.

**General description of harmonic radar system**

The harmonic radar system is shown in the block diagram of Fig. 6. A varactor-tuned transferred-electron oscillator (t.e.o.) generates c.w. power at X-band. A triangular waveform is used to frequency modulate the t.e.o. with a total frequency excursion of  $\Delta F$  at a rate of  $f_m$  as shown in Fig. 7. The frequency-swept power is radiated from antenna  $A_1$  mounted on the front of the trailing car (see Fig. 6). This power impinges on a similar antenna  $A_2$  which is a part of the harmonic reflector mounted on the back of the front car. The passive doubler generates the second harmonic frequency of the power incident on

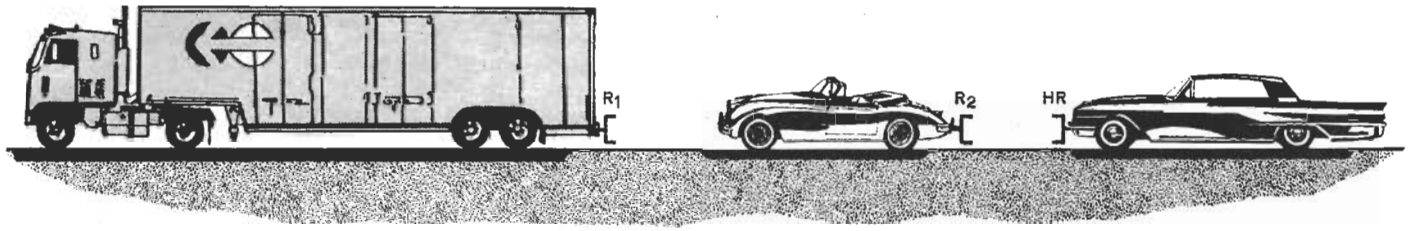


Fig. 5. Conventional versus harmonic radar: masking.

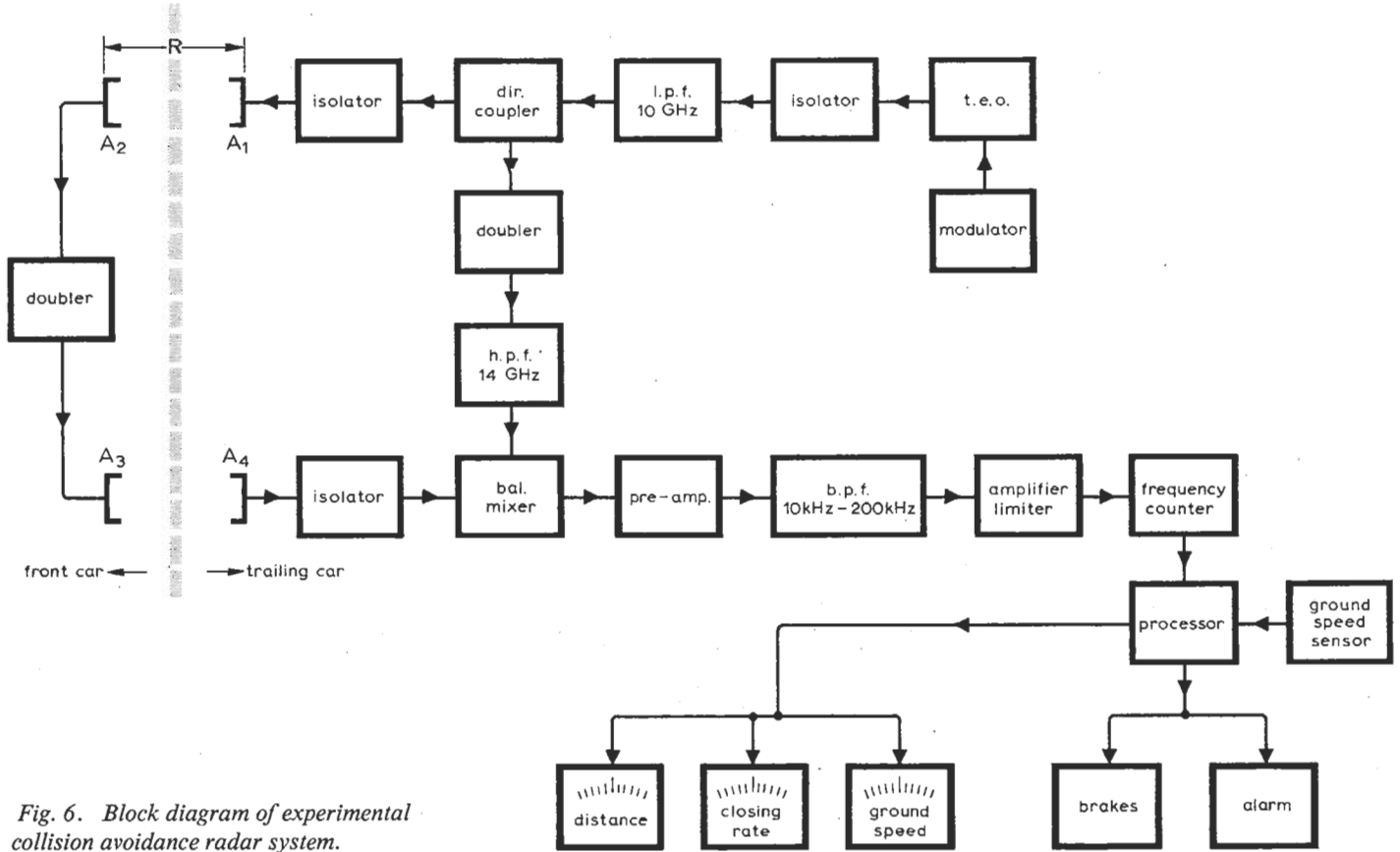


Fig. 6. Block diagram of experimental collision avoidance radar system.

antenna A<sub>2</sub> and radiates it back to the trailing car via antenna A<sub>3</sub>. This frequency is in Ku-band. The receiving antenna A<sub>4</sub> delivers the received power, which is at the second harmonic frequency, to the mixer, where it is mixed with a sample of the doubled frequency of the transmitter power.

The returned signal is shifted in frequency from the second harmonic of the transmitted frequency due to the round trip time delay  $\tau = 2R/c$  ( $R$  is the distance between cars and  $c$  is the velocity of light). The frequency shift (or difference frequency,  $f_R$ ) is given by

$$f_R = \frac{df}{dt} \cdot \tau = \frac{8\Delta F f_m R}{c}$$

A measurement of the frequency shift yields the range since the time delay is proportional to the distance between cars.

Two techniques for measuring this frequency shift have been investigated for the automotive radar. The first, for which the bulk of the experimental effort has been carried out, will be described first.

The output of the mixer is amplified, filtered and then fed into a counting

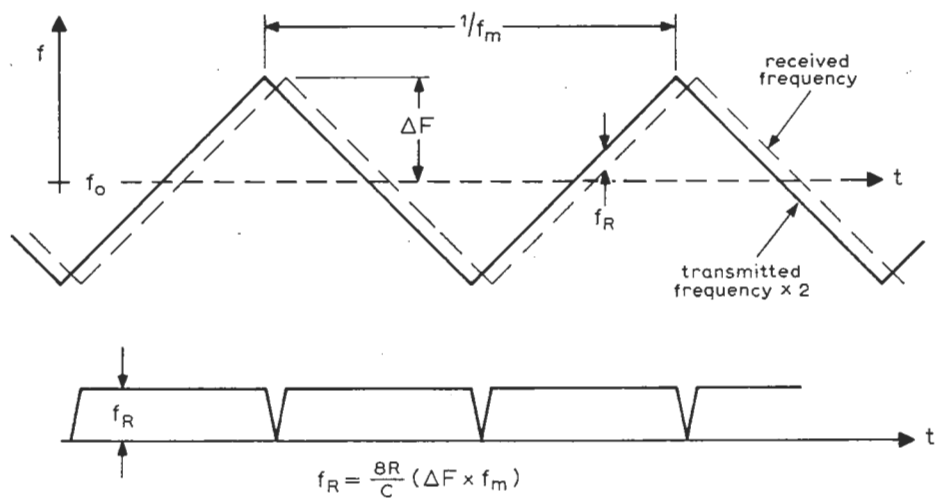


Fig. 7. Modulation scheme of harmonic radar.

circuit. This counting circuit develops a voltage which is proportional to the rate of zero crossings of the input signal and therefore the range. In addition, the radar processing circuitry derives a voltage which is proportional to the first derivative of the range, i.e., the closing rate. To make a

proper decision for a "safe distance", a third piece of information—the ground speed of the vehicle—is used. The ground speed is derived from an independent microwave Doppler speed sensor. The radar processor combines the three measurements of range, closing rate and

ground speed in a predetermined fashion, depending on the criteria chosen for "safe distance", which are, of course, dependent on weather and road conditions. When a dangerous driving situation is detected, an audible warning is sounded and a light is flashed. In our experimental unit, with the system switched to the automatic braking mode, the brakes are also applied for dangerous driving situations. The range, closing rate and ground speed are displayed on three panel meters mounted on the dashboard. In an operational system, it is not expected that these measured quantities would be displayed.

### Quantization effects

As shown in Fig. 7, the difference frequency  $f_R$  is given by

$$f_R = 8\Delta F f_m R/c \quad (1)$$

where  $R$  is the distance between vehicles,  $\Delta F$  is the total frequency excursion at X-band, and  $f_m$  is the modulation frequency. The choice of parameters  $\Delta F$  and  $f_m$  is closely related to the presence of a step error (or quantization error) in distance

measurements with frequency modulated radar. The conventional signal processing technique<sup>2</sup> which measures the return frequency by counting the number of zero crossings that occur within a fixed time interval leads to a result which is quantized in frequency and therefore in range. The quantization arises because the difference frequency waveform is periodic in  $f_m$ . Therefore the average measured frequency (as measured by using the entire waveform and counting zero crossings in a fixed time interval) must be a multiple of  $f_m$ . The quantization step in range  $\Delta R$  is therefore (from equation (1)) equal to

$$\Delta R = c/8\Delta F$$

To minimize this basic "granularity" in distance readings,  $\Delta F$  should be chosen as large as possible. In practice, bandwidth limitations in the doubler and mixing circuits, as well as regulations requiring the efficient use of frequency spectrum do not allow  $\Delta F$  to exceed a few tens of MHz. In the experimental system, a good compromise was found to be  $\Delta F$  equal to 25MHz, resulting in a range quantization of 1.5 metres. This quantization error can

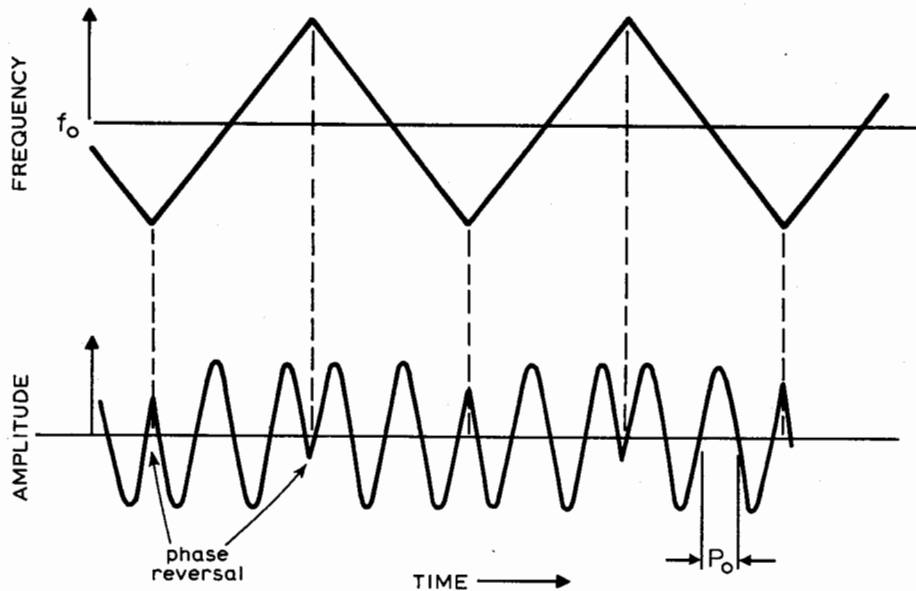


Fig. 8. Typical difference frequency waveform.

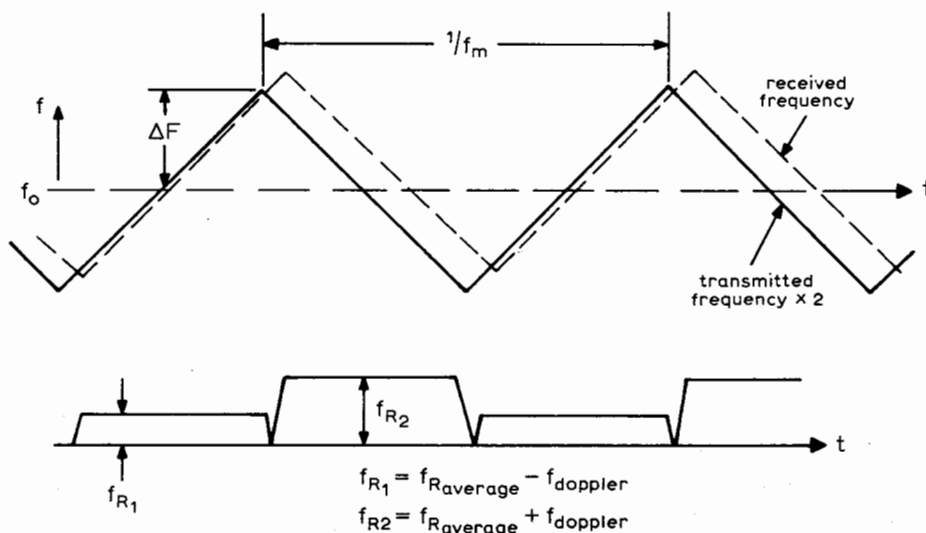


Fig. 9. Doppler shifts with moving vehicles.

be tolerated in a distance measurement for collision avoidance where the relative motion of the two vehicles tends to have an error-smoothing effect.

A different processing technique has also been investigated. This technique processes the difference frequency waveform in a digital manner allowing accurate range measurements to be made without the quantization limitation just described. This technique can allow the radar to operate with a smaller frequency deviation  $\Delta F$  which in turn simplifies the bandwidth requirements at the t.e.o., mixer, doubler etc., as well as conserving r.f. spectrum.

To understand how this signal processor overcomes the quantization limitation refer to Fig. 8, which depicts a typical difference frequency versus time waveform. The number of zero crossings in a given time interval is quantized, with the quantization effects arising because of the phase reversals occurring every  $1/2f_m$  seconds. However, if we restrict our attention to portions of the difference frequency waveform that are removed from the phase reversals, then we see that the time between zero crossings of this restricted portion of the waveform is not quantized.

If an accurate measurement of this time period ( $p_0$ ) were made, then a non-quantized frequency ( $1/2p_0$ ) could be found by generating the reciprocal of the measured period. This non-quantized frequency could then be converted to range via the relationship shown in eq. (1). Further details of the non-quantized signal processing technique are presented in the video circuits and signal processing sections of this paper.

### Modulation parameters

The frequency excursion at X-band is 25MHz while the modulation frequency is 3kHz. This was chosen as a compromise because if  $f_m$  is made very high, the video bandwidth needed to accommodate the expected variation in range becomes very large while if  $f_m$  is made very low, there are various components of noise (in excess of thermal noise) which behave as  $1/f$  noise limiting system performance. For the parameters chosen, the frequency versus range slope is 2kHz/m resulting in a 10kHz-200kHz range for the difference frequency as the distance varies from 5 to 100 metres.

### Doppler shifts

As seen in Fig. 9, relative movement between vehicles will have the effect of shifting the difference frequency by an amount equal to the Doppler frequency. It will be a positive shift during one half of the modulation cycle and an equal but negative shift during the other half. The average difference frequency (averaged over many cycles of  $f_m$ ) will be the same as for a stationary car at the same average distance. The range reading is therefore independent of the Doppler shifts. An up-down counter switched in synchronism with  $f_m$  could be used to detect the closing rate. In the present system, however, the closing rate is derived by differentiation of  $F$

## Frequency doubler

The success of the harmonic radar concept was critically dependent on developing an efficient, passive harmonic reflector, i.e., finding a solid-state device which in a suitable circuit will generate the second harmonic with the required efficiency. For the car radar application it was felt strongly that the reflector must be completely passive, with no wiring to the car's electrical system to insure reliable operation and inexpensive installation.

The above needs have been met by the device shown in Photo 1. A silicon Schottky barrier diode is mounted in a microstrip circuit. A 0.8thou'-diameter diode chip is seen connected across a gap, located for best impedance match in a  $\lambda/2$  (fundamental resonator). Input at X-band is coupled at a voltage maximum point of the fundamental frequency, output is coupled at a voltage maximum point of the second harmonic, with a  $\lambda/4$  open section coupled to the output line to reflect the fundamental frequency back into the circuit. Fig. 10 shows the conversion efficiency of the doubler circuit. As one would expect, at the lower levels the power output at the second harmonic varies as the square of the power input at the fundamental, following a law of

$$P_{out} = KP_{in}^2$$

with  $K$  equal to  $2500 W^{-1}$ . The bandwidth of the doubler is approximately 75MHz, centred within the Ku-band in the experimental unit.

A similar doubler circuit is used to provide a sample of double frequency transmitter power to the local oscillator port of the mixer, but this circuit is operating at high power levels. A 50mW input at X-band yields a conversion efficiency of 10% over a 200MHz band.

## Antennas

The choice of antennas and the r.f. frequency are closely related. For reasonable traffic-lane discrimination, a maximum horizontal beamwidth of  $5^\circ$  requires a horizontal aperture width of ten wavelengths. To achieve this aperture in a 12in physical size (approximately licence plate size) necessarily places us somewhere in X-band. A  $10\lambda \times 10\lambda$  aperture with 50% efficiency has a gain of 28dB, which makes transmitter power requirements quite reasonable. Also, solid-state power sources at X-band frequencies are readily available, and spectrum space at X-band is still under-utilized.

Printed antenna design was found quite suitable for our system. The X-band antenna has an aperture of  $13 \times 7\frac{1}{2}$ in, a gain of 26dB at 9GHz, and a 10% bandwidth. It consists of 128 fan-shaped dipoles printed on both sides of a 1/32-in thick polyethylene sheet, phased into a 50 $\Omega$  input through a succession of quarter-wave balanced transmission lines. An 18GHz antenna has been produced by scaling up in frequency from the X-band design, with similar electrical characteristics.

By using a polarization of the Ku-band antenna at  $90^\circ$  to the polarization of the

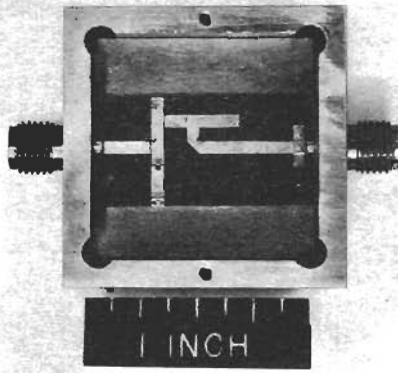


Photo 1. Frequency doubler microstrip circuit.

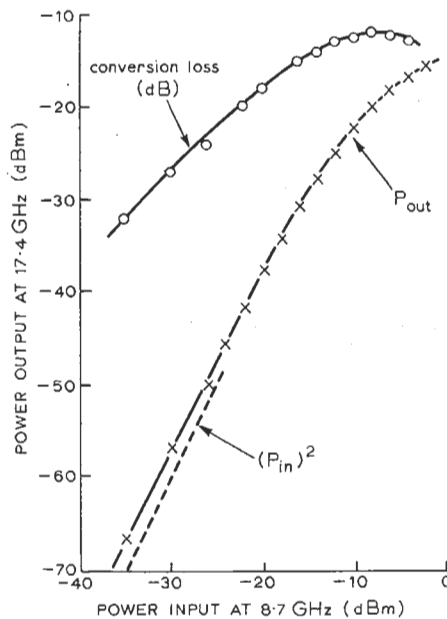


Fig. 10. Harmonic generation efficiency of frequency doubler.

X-band antenna, we get additional rejection of spurious second harmonic power generated at the source and received either directly from an oncoming vehicle or reflected from "nontagged" objects. This is in addition to second-harmonic filtering at the low-pass filter and isolators in the transmitter circuit. Total rejection of spurious second harmonic amounts to 150dB, reducing it to well below receiver noise level.

## Doppler speed sensor

A low-power microwave Doppler speed sensor was developed for use on cars and lorries to provide true ground speed for both anti-skid braking and speedometer applications. In an anti-skid system, the true ground speed and wheel speed are compared to accurately determine wheel slip during braking.

The speed sensor, which is shown in photo 2 and diagrammatically in Fig. 11, is a completely self-contained radar including transmitter, receiver, antenna, d.c. and signal processing circuits. A smaller version of the printed antenna in the collision avoidance radar is used for transmitting to and receiving signals from the road surface. The radar is mounted on the vehicle so that the beam lies in a vertical plane, with the vehicle's velocity vector at an acute angle  $\theta$  (typically  $45^\circ$ ) to the road surface. Part of the transmitted signal is diffusely reflected from the road surface back to the antenna. If the vehicle is moving with a velocity  $v$ , the reflected signal is shifted by the Doppler effect and the difference between transmitted and reflected frequencies is given by  $F_D = 2v \cos\theta/\tau$  where  $\tau$  is the wavelength of the transmitted signal. This difference frequency is extracted from the mixer and is converted to a series of fixed width pulses having a repetition rate proportional to speed. The pulses may be counted to indicate total distance or may be averaged for analogue speed information as is the case for the collision avoidance system. These radar speedometers have an operating

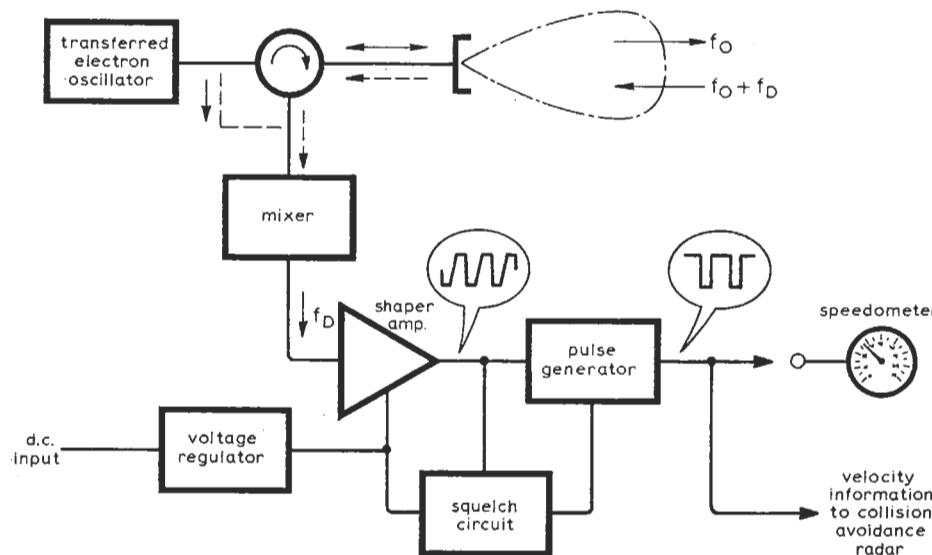


Fig. 11. Block diagram of Doppler radar module.

temperature range of -60 to +75°C and, once calibrated, have demonstrated inaccuracies of about 1% or less on dry road surfaces for speeds of 20-70 m.p.h.

**Signal propagation**

Assuming free-space propagation conditions, effective antenna apertures of  $A_f$  and  $A_{2f}$  for the X-band and Ku-band antennas, respectively, a target at distance  $R$  will present to the receiver a signal power of

$$P_r = (4K)P_0^2 A_f^4 A_{2f}^2 / \lambda^6 R^6 \quad (2)$$

where  $P_0$  is the transmitter power at the fundamental wavelength  $\lambda$  and  $K$  is the doubler coefficient when operating in its square law region where  $P_{out}$  equals  $K(P_{in})^2$ .

The signal strength at the receiver is modified by ground reflections. Power will reach the antennas via a ground reflection in addition to the direct path. For the car, radar angles of incidence are between 5° and 0.5°. At such small angles, the reflection coefficients for horizontal and vertical polarization are similar (about 0.7 to 0.8 in magnitude and a phase shift of close to  $\pi$  radians). As a result of the ground reflected component, the range equation (2) has to be modified. Assuming an ideal case (not far from reality) where the reflection coefficient is equal to -1,

$$P_r' = P_r [64 \sin^4 (2\pi h_1 h_2 / \lambda R) \times \sin^2 (4\pi h_1 h_2 / \lambda R)] \quad (3)$$

where  $h_1, h_2$  are heights above ground of the active radar and passive reflector antennas, respectively, and  $\lambda$  is the fundamental wavelength. As  $R$  changes, we expect a series of reinforcements and partial cancellations of signal strength. A partial cancellation will occur wherever  $R = 4h_1 h_2 / n\lambda$ , where  $n = 1, 2, 3 \dots$  and for the values  $h_1 = h_2 = 0.52m$  of the experimental radar. A signal minimum is expected at  $R_{n=1}$  equals 32m and  $R_{n=2}$  equal to 16m, with more below  $R_{min}$ .

For distances where  $R > 10h_1 h_2 / \lambda$ , the trigonometric functions in eq. (3) can be replaced by the arguments, resulting in a received signal of

$$P_r'' \propto P_0^2 A_f^4 A_{2f}^2 (h_1 h_2)^6 / (\lambda R)^{12}$$

indicating a drop-off with distance as steep as  $R^{-12}$ .

It is obviously more advantageous, relative to conventional radar systems, to increase the source power, and, for a given total aperture, to allocate the larger area to the fundamental antenna. In our radar, this aperture ratio is 4:1, giving the same gain to the two antennas. The very steep decrease of signal strength with distance has an advantage in that interference effects caused by out-of-range targets will be greatly reduced.

Measured signal strength as a function of distance is shown in Fig. 12 for the experimental radar over dry asphalt.

**Source of noise**

There are several sources of noise in the present radar system which limit the range. These sources include thermal noise, essentially "white" across the system-bandwidth

$$B = f_{Rmax} - f_{Rmin}$$

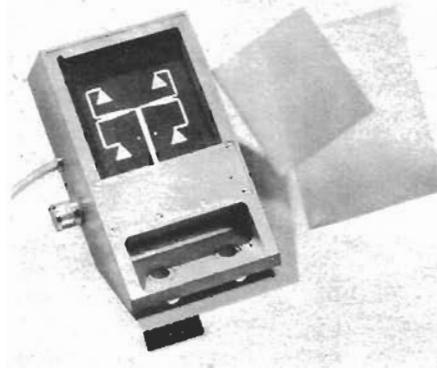


Photo 2. Doppler ground speed radar.

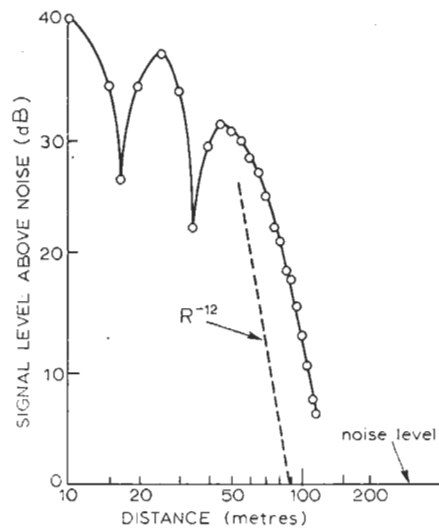


Fig. 12. Signal strength versus distance. (Antenna is 21in above road surface.)

Local oscillator noise, generated by beat products of the t.e.o. noise spectrum in a bandwidth  $B$  away from the carrier<sup>3,4</sup>. This noise source varies with the "corner" at  $f = 100kHz$ . It is possible to reduce the effects of noise source by using a balanced mixer. For the radar parameters, with a mixer balance reduction of 20dB, the local oscillator noise becomes less than thermal. Amplitude modulation at the local oscillator, caused by the dependence of t.e.o. output power on frequency as frequency is varied over a range  $\Delta F$ . This noise source has frequency components at  $f_m$  and its harmonics. Use of a balanced mixer and a t.e.o. power variation of less than 0.1dB over  $\Delta F$  ensure that this noise source is of minor importance. Mixer sensitivity and balance are strongly dependent on frequency. This is partly caused by the fact that the isolation between the r.f. ports is rather poor (~ 6dB), causing multiple reflections of the local oscillator power and its harmonics at the imperfectly matched isolator, antenna, and high-pass filter (see Fig. 6). When swept over a range of frequencies  $\Delta F$ , a noise signal at  $f_m$  is generated at the i.f. output port, the harmonics of which enter the video band,  $f_{Rmin}$  to  $f_{Rmax}$  of the system. The magnitude of this noise signal varies with the mixer diodes in use and the

choice of centre frequency. With careful matching of components and adjustment of cable lengths it can be reduced, but in practice it is the dominant noise source, exceeding the first two contributions by 10-20dB. Therefore, the current design is not operating at its theoretical Johnson noise limit regarding signal-to-noise ratios, and consequently its maximum range of 100m is below a theoretical noise limited system.

Improvement in the future can be achieved by using a balanced mixer design which has better isolation and is less prone to generating spurious signals at  $f_m$  and its harmonics. One could also attempt matched filtering in the video amplifier chain to improve matching between the amplitude and range characteristic of the radar system. Should increased range become necessary a more sophisticated and complex design may be used, incorporating a tracking, narrow-band filter.

In the present design, a signal of  $P_{min}$  equal to -80dBm is required at the receiver input for a 10dB overall s/n ratio.

(To be continued)

**References**

1. "Accident Facts", published by National Safety Council, Chicago, Ill., 1971 Edition.
2. Luck, D. G. C., "Frequency Modulation Radar", McGraw-Hill (1949).
3. Narayan, S. Y., and Sterzer, F., "Transferred Electron Amplifiers and Oscillators," *IEEE Trans. on Microwave Theory and Techniques* (November 1970).
4. Ohtomo, M., "Experimental Evaluation of Noise Parameters in Gunn and Avalanche Oscillators", *IEEE Trans. on Microwave Theory and Techniques* (July 1972).

**Sixty Years Ago**

In these days of "light current" electronics, and the professional, highly qualified radio engineer, it is worth remembering that it was not always thus. This extract from *Wireless World*, May 1914, may give some inkling of the sort of thing your average engineer came up against.

'Wireless Engineer' sends us the following two recipes for a cheap mixture for covering boilers in order to prevent loss of heat:

(1) Take 1 bushel of fireclay, 1 bushel of ordinary clay, 1 bushel of cow-dung, 1/2 bushel of ashes (not the finest dust), 1/2 gal. of coal-tar, and a little plasterers' hair as a binder; mix well together . . ."

And now we grumble when integrated circuits are in short supply!

# Clutter-free radar for cars

## Conclusion: frequency measurement and application

by J. Shefer, R. J. Klensch, G. Kaplan and H. C. Johnson

RCA Laboratories, New Jersey

As described in last month's section on quantization there have been two different approaches to frequency measurement designed and tested for the automotive radar. One uses the rate of zero crossings counting technique and the other uses the average period measurement technique. Both techniques will be described although most of the experimental effort has been concentrated on the conventional counting technique.

### Video circuits and signal processing

Following pre-amplification and the 10kHz band pass filter is a high-level amplifier/clipper which clips signals about 2 or 3dB above the background level. The conventional counter consists of a one-shot circuit that is triggered by the clipped input signal. The duration of the one-shot "on" time is as long as possible, consistent with the maximum input signal frequency of 200kHz. Making the "on" time as long as possible gives the most noise immunity possible since this particular one-shot cannot be retriggered during its "on" time. If the output of the one-shot is integrated then a voltage proportional to its range is obtained. Likewise, if the one-shot is made to drive a meter movement, the deflection will be proportional to range. Such a meter has been connected and calibrated to read 100 metres at full scale.

In a collision avoidance system more than just the range to the car in front is needed. Some velocity data must be used in conjunction with the range so that a decision can be made to slow down or continue. Velocity data is obtained from a Doppler speed sensor. By integrating the output pulse train of the Doppler unit a voltage proportional to velocity is developed, which is displayed on a second meter, calibrated in miles-per-hour with a full scale of 100m.p.h. Combining the two signals (range and velocity) in a variable threshold device, it is possible to sound an alarm whenever the vehicle gets too close to the car in front for the speed being maintained. One car length for each 10m.p.h. of velocity is an example for a typical alarm setting, which may be set to any desired value.

There exists one other useful bit of information in determining the presence of a hazard. It is the closing velocity between

the two vehicles in question. Knowing the closing velocity as well as the range between vehicles and one's own velocity, it is possible to further optimize the condition for giving the danger signal. In the experimental radar, the alarm is sounded and the brakes are applied when

$$R < (k_1 v + k_2 dR/dt) \dots (4)$$

where  $R$  is the distance between vehicles,  $v$  is the velocity of the following vehicle,  $dR/dt$  is the closing velocity between the two vehicles,  $k_1$  is the factor mentioned earlier, such as one car length per 10m.p.h. or 0.5 metres/m.p.h. and  $k_2$  is a factor, determined by trial and error to be in the region between 1 and 3 metres/m.p.h.

If the closing velocity,  $dR/dt$  were not available, eq. (4) would reduce to  $R < k_1 V$  for the alarm to be given. The constant  $k_1$  would have to be made large enough to allow a safe stop for the situation of a car closing on a parked car. However, for the condition of the two moving vehicles (one following the other) the system would then appear to be overconservative. By adding the  $dR/dt$  factor, the system recognizes closing velocity and thereby allow  $k_1$  to be made smaller, the assumption being that the car in front cannot come to a sudden stop but must decelerate. This deceleration would appear as an increase in closing velocity which would cause the following car to also decelerate so both cars would then stop safely.

It should be noted that provisions can easily be made for the driver to reset, by the "flick of a switch", constants  $k_1$  and  $k_2$  in accordance with prevailing weather and road conditions.

The closing rate,  $dR/dt$ , can be derived

either by differentiating the range voltage,  $R$ , or by obtaining the Doppler shift directly from the video signal. As seen from Fig. 9, if a switched up-down counter is used, synchronous with the triangular modulation,  $f_m$ , a count proportional to the Doppler shift can be obtained.

The first of these methods was used in the experimental model, using a capacitor-driven operational amplifier with resistive negative feedback. A third meter, calibrated in m.p.h., displays the negative (receding) or positive (approaching) closing rates, and the alarm circuit utilizes  $dR/dt$  according to eq. (4).

The processing system which eliminates the quantization effects is outlined in Fig. 13. There are several main blocks shown in this figure. The first block selects a suitable portion of the difference frequency waveform to use for the measurement. It is important that the phase reversal portions (shown in Fig. 8) not be included within the measurement because of the quantization effects that are caused by the phase reversals occurring near the peaks and valleys of the triangular modulation waveform. A suitable portion of the difference frequency waveform must always fall between these peaks and valleys. It is also desirable to utilize a large fraction of the difference frequency waveform so that the measurement will be reliable and the effects of noise are averaged. Therefore, we want to use a sampling of the waveform that consists of at least a minimum duration interval for reliable processing and noise immunity but is not too large so that the phase reversal portions of the waveform are not excluded.

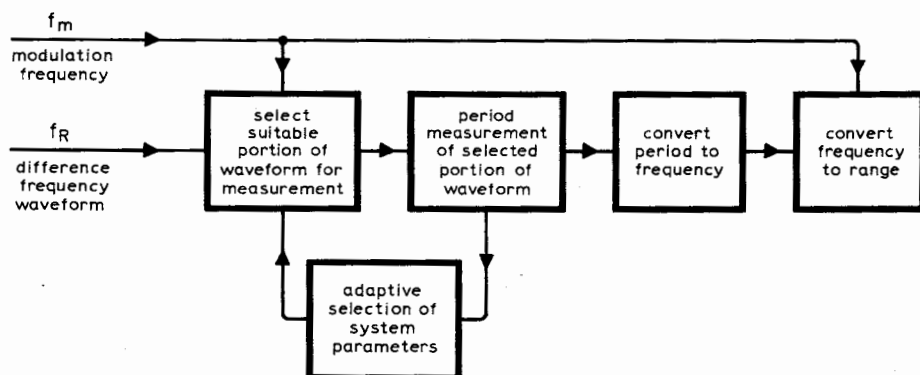


Fig. 13. Outline of non-quantized measurement system.

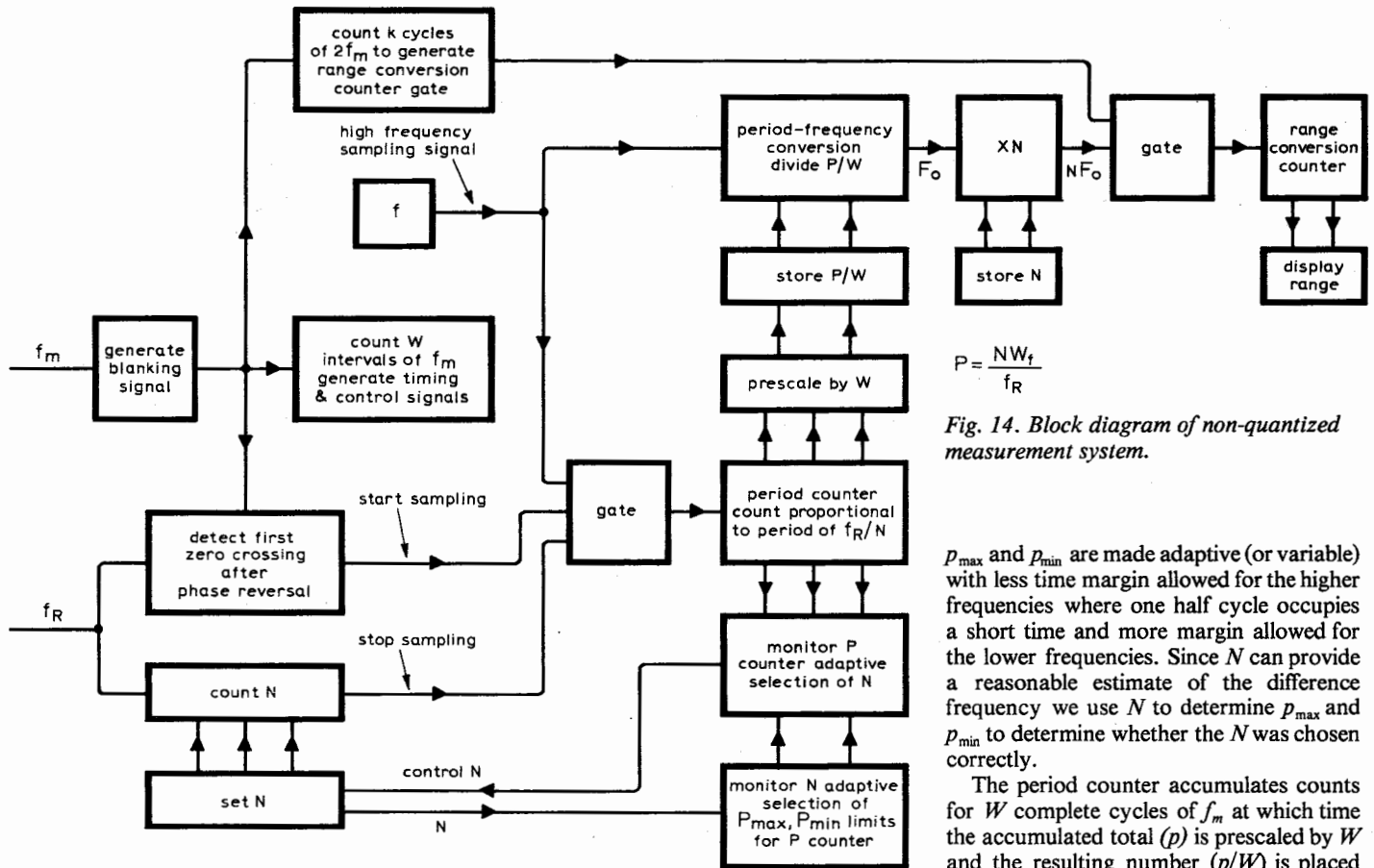


Fig. 14. Block diagram of non-quantized measurement system.

The difference frequency is not constrained to stay within a narrow range but will vary (perhaps over a 20:1 ratio or more). Therefore, to best accommodate the wide dynamic range of difference frequencies, the measurement system is an adaptive one. That is, the system's parameters are allowed to change as the difference frequency changes in a way which achieves the "goal" of selecting a suitable portion of the waveform for processing. A decision to change the measurement parameters is made by monitoring the period measurement and taking appropriate action to adjust the measurement parameters. This will be more fully described below. As shown in Fig. 13, the next steps are to convert the period measurement to a frequency and then to a range. A more detailed system diagram is shown in Fig. 14.

Inputs to the processor are the difference frequency waveform and the triangular modulation waveform of frequency  $f_m$ . From the triangular modulation waveform, a pulse train, of frequency  $2f_m$  and called the blanking signal, is generated with a pulse occurring at the peaks and valleys of the modulation waveform.

The period measurement begins by detecting the first zero crossing of the difference frequency waveform that occurs after the end of a blanking signal pulse. This insures that the phase reversal of the difference frequency waveform is completed before the measurement begins. At the time of this zero crossing, a high-frequency pulse train of frequency  $f$  pulses per second is gated into a counter called the period counter. After  $N$  additional zero crossings (half cycles) of the difference

frequency waveform have occurred, the gate is closed and the counter stops incrementing. The process is repeated after the next blanking signal occurs and continues for a total of  $2W$  blanking pulses. At this time the count ( $p$ ) in the period counter is given by (5)

$$p = \frac{WNf}{f_R} \dots \dots \dots (5)$$

For reliable measurements,  $N$  must be chosen correctly. If  $N$  is too large, the sampling interval can extend beyond the next blanking signal into the phase reversal region, while if  $N$  is too small, the measurement will not be accurate because useful information is discarded. By monitoring the period counter outputs, we can determine the average sampling time. If the sampling time is too small, then the processor increases  $N$  for the next measurement, if the sampling time is too long, then  $N$  will be decreased for the next measurement. Basically we monitor the period counter, compare its contents with two limits,  $p_{max}$  and  $p_{min}$ , and have the processor always adjusting  $N$  to maintain the period counter output between these limits.

The time of the first zero crossing of the difference frequency may vary by up to one half cycle of the difference frequency. Therefore, in choosing  $p_{max}$ , a safety margin must be allowed for, with the safety margin being larger for the low frequencies. Because the difference frequency varies (in frequency) over a wide range, a safety margin that is adequate for the lower frequencies is excessive for the higher frequencies. To make better use of the difference frequency waveform, the limits

$p_{max}$  and  $p_{min}$  are made adaptive (or variable) with less time margin allowed for the higher frequencies where one half cycle occupies a short time and more margin allowed for the lower frequencies. Since  $N$  can provide a reasonable estimate of the difference frequency we use  $N$  to determine  $p_{max}$  and  $p_{min}$  to determine whether the  $N$  was chosen correctly.

The period counter accumulates counts for  $W$  complete cycles of  $f_m$  at which time the accumulated total ( $p$ ) is prescaled by  $W$  and the resulting number ( $p/W$ ) is placed in a storage register. The value of  $N$  that was used for the measurement is also stored. If a change to a new value for  $N$  is made, the counters are reset and a new period measurement is started.

The processor now begins to convert the period measurement to a frequency. As shown in Fig. 14, the first step in this conversion is to strobe the scaled ( $p/W$ ) count into a pre-settable centre operating in the down count mode. The clock input to the counter is the same high-frequency sampling pulse train used to measure the period. The output from this period conversion counter is a pulse train of frequency  $f_0$  where

$$f_0 = \frac{f}{p/W} = \frac{f_R}{N}$$

The output frequency ( $f_0$ ) is then fed into a circuit which generates  $N$  output pulses for each input pulse. The new output frequency ( $Nf_0$ ) is then equal to  $f_R$ .

By using the same pulse train ( $f$ ) to generate counts in the period counter and then to convert the measured period to a frequency, we have made the frequency stability of the sampling pulse train relatively unimportant.

So far we have measured the period of the difference frequency waveform excluding the phase reversal portions and have converted this period measurement into a pulse train of the same frequency as the input frequency. However, by excluding the phase reversal region from the measurements, we insure that the output frequency is not subject to the coarse quantization effect that arises with conventional processing. A conversion of frequency to range is made by first generating a time gate of



duration  $K/2f_m$  and then gating the output frequency  $Nf_0$  into the range conversion counter. The range conversion counter has a count of  $(4\Delta FK/c)R$  accumulated and by setting  $4\Delta FK/c$  equal to a convenient number such as 10, each count equals 0.1 metres. A display is easily driven if the range conversion counter is arranged as a cascade of decode counters. Note that by generating a range conversion gate from  $f_m$ , any variation or drift in  $f_m$  is automatically compensated for in the range measurement.

The processor just described does not require any accurate clocks within the processing system. Frequency variations in the high-frequency sampling pulse train are compensated for by using the same pulse train for period measurements and period-to-frequency conversion. Also variations in  $f_m$  are compensated for by using  $f_m$  to generate the range conversion counter time gate.

**Automatic collision avoidance braking**

The automatic braking system in the experimental radar is fairly rudimentary at the moment in that once the alarm is given, the brake pedal is automatically depressed by a force that increases linearly with time to maximum pressure, until the alarm is removed. The force is then removed linearly with time. Developing the force necessary to apply the brakes was accomplished by using a vacuum-operated piston. The piston pulls the pedal via a spring in series with a flexible cable that goes through the bulk-head and connects to the brake pedal. This allows the driver to override or augment the braking if necessary. The valve that allows the engine's vacuum system to evacuate the chamber of the piston is driven by electrical signals derived from the signal processor when an alarm is given.

A proportional braking system is currently under consideration where the brakes will be applied according to the severity of the danger situation; the pedal force  $P$  will then be

$$P = k_p [K_1 v + k_2 (dR/dt) - R]$$

where  $k_p$  is a constant, adjusted to the car's braking and accelerating dynamics, and has the dimensions of force/metre.

**Experimental tests**

The experimental system uses an RCA transferred electron oscillator power source. Antennas are modified and scaled versions of the RCA hand-held radar. An efficient doubler circuit in microstrip was developed at RCA Laboratories, as well as the various video circuits for amplification, filtering and processing. Other r.f. components were purchased as standard catalogue items.

The components of the experimental system include the Doppler speed sensor and the active radar power supply which operates from the 12-volt car battery. The maximum power drain is 20W. The reflector is completely passive and therefore needs no power.

The experimental set-up on the test vehicle is shown in Photos 3 and 4. Although the active radar and passive reflector are slightly larger than an American licence plate, scaling to higher frequen-

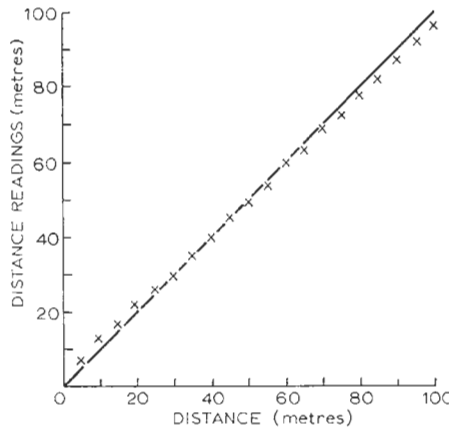


Fig. 15. Accuracy of distance measurements.

cies would decrease the size to that of a licence plate. The registration numbers can then be imprinted on the protective antenna covers, (glassfibre) and the units can be mounted in the space reserved for licence plates. Alternatively, the active radar can be mounted behind a plastic grille.

The experimental collision avoidance radar has been extensively tested on RCA Laboratories' grounds and adjoining highways. Although not specifically

"ruggedized" for highway use, the system has not failed from vibrations or adverse climatic conditions. It was not affected by rain appreciably, nor was the performance noticeably degraded by applying a layer of mud and road dirt to the antenna covers.

The distance measurements were quite repeatable and of adequate accuracy. Fig. 15 shows measurements of distance readings on the display meter versus actual distances (using the zero crossings counting technique). Errors can be reduced further by using a more linear meter movement although the quantization limitation is still present.

Experimental tests were concerned with determining whether the new processor would not be subject to the coarse quantization effects that previously occurred. The radar and processor were mounted on a car which was situated 40 metres from the harmonic reflector. Then the car was slowly moved in 0.1-metre increments a total of 1.5 metres. At each point a reading on a digital display was noted (the display itself had a quantization of 0.1 metres). The experimental parameters of the system were  $f_m = 2.2\text{kHz}$  and  $\Delta F = 22\text{MHz}$ . For these parameters, the quantization error with the zero crossing processing previously used was about 1.7 metres. Results of the experiment using the new processing

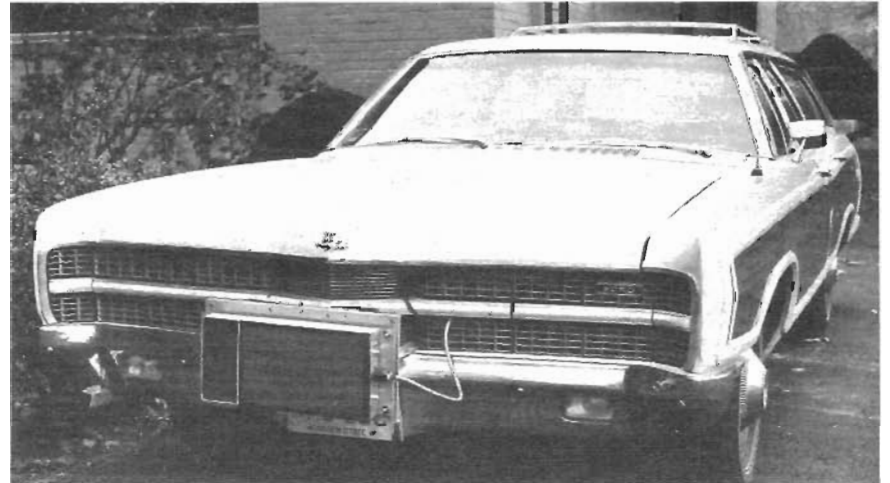


Photo 3. Active part of experimental radar.

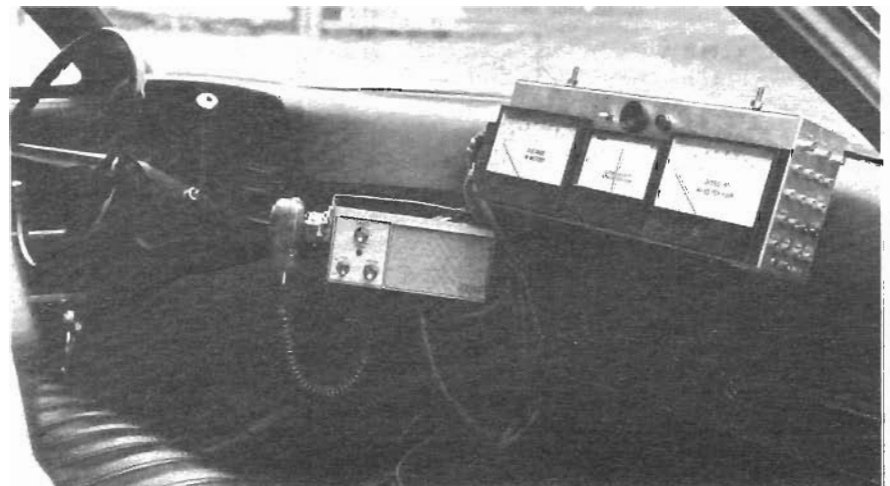


Photo 4. Processing and display unit inside vehicle.

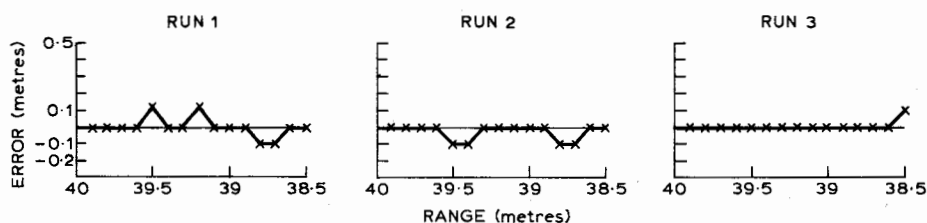


Fig. 16. Experimental results with non-quantized processing.

technique are shown in Fig. 16. Note that the quantization has been reduced to 0.1 metres (basically the display limitation). Therefore, the new technique does eliminate the coarse quantization effect.

### Modes of operation

Several different modes of utilizing the collision avoidance radar can be discerned. In a semi-automatic mode, the radar will sound and flash an alarm whenever warranted; taking action will be left to the driver, who may choose to slow down, change lanes, or ignore the warning for any reason.

In another mode of operation, the brakes can be applied automatically, either immediately the alarm is sounded, or with delayed action, giving the driver a chance to act first. If the driver fails to act, the system will provide a last-minute "panic" stop that will at least moderate the collision impact.

In yet another mode, the collision avoidance radar can be integrated with a cruise control system, providing completely "foot off" operation.

It is also possible to "tag" specifically identified collision hazards located on or off the highway, such as bridge abutments, construction barriers or trees. A reflector mounted on such an obstacle will stop a car approaching it within a predetermined angle, but will not influence a car travelling in a safe lane.

Reflectors can also be placed at wrong-way entrances to one-way streets or highway exit ramps to prevent inadvertent entry.

### Cost and cost effectiveness

The system lends itself very well to integration using printed-circuit techniques throughout. The passive reflector, which in general use will have to be mounted by law on the back of every vehicle (similar to requirements of red tail-lights), can be produced inexpensively on one printed-circuit board. The active radar is more complex, but not more than a.m./f.m. radios currently used in cars.

To make the radar "cost effective", its cost must be less than the damage involved in the rear-end collisions which have been prevented through its use, on the average. We have mentioned an estimate of \$10 billion in "societal cost" per year due to rear-end collisions. This comes to \$100 per car per year, which amounts to a substantial sum over a vehicle's lifetime. A radar with a capability of preventing or moderating even a fraction of the rear-end collision damage might become quite an attractive proposition.

### Acknowledgements

The harmonic radar effort has drawn on the talents and skills of diverse RCA groups. The authors are grateful to Harold Staras, who held the whole project together and provided ideas and encouragement at every turn; to L. Schiff for many fruitful discussions; to W. C. Wilkinson, O. M. Woodward and Z. L. White who designed and constructed the antennas; to L. S. Napoli, J. J. Hughes and J. Rosen who developed the microstrip doubler circuit; A. Presser who designed the local oscillator doubler; and to R. Burgen and T. Nolan who helped build and road-test the system and A. Ritzie who constructed the new processor and aided in the testing.